through the TAK1–NLK kinase pathway involving STAT3 as a scaffold (Kojima *et al.* 2005), although the levels of pY705 were much lower and rapidly decreased in both STAT3WT and STAT3S727A under stimulation with G108YRHQ.

To understand the role of phosphorylation at Ser727, we examined the effects of phosphorylation at Ser727 itself in addition to the mutants shown above. We previously showed that the pretreatment of HepG2 with a protein kinase inhibitor H7 and a MEK inhibitor PD98059 greatly inhibited the IL-6-induced Ser727 phosphorylation of STAT3 as well as its accompanying mobility shifts (Abe *et al.* 2001). To test whether Ser727 phosphorylation with mobility shifts is involved in the rapid dephosphory lation of pY705 in STAT3WT, we examined the dephosphorylation of pY705 in the presence of H7 and PD98059. As shown in Fig. 3D, IL-6 rapidly caused tyrosine phosphorylation at Y705 and an increase in the level of pS727 together with apparent mobility shifts of STAT3WT at 15 min. Transient activation of ERK1/2 was detected with anti-phosphoERK at 15 min. Pretreatment with H7 plus PD98059 mostly inhibited both the increases in Ser727 phosphorylation and the mobility shifts. This treatment significantly diminished the rate of pY705 dephosphorylation compared with that in the absence of those inhibitors. The rate of dephosphorylation of pY705 in the presence of H7 plus PD98059 did not match that of STAT3S727A. This difference may result from the incomplete inhibition of S727 phosphorylation with mobility shifts by these inhibitors. Taken together, these data indicate that the phosphorylation of Ser727 is likely to be required for the rapid dephosphorylation of pY705 of STAT3.

Phospho-Ser727-dependent decrease in pY705 is largely mediated by TC45

Next, we searched for the tyrosine phosphatase that is responsible for the phospho-Ser727-dependent dephosphorylation of STAT3 pY705. To date, several PTPs have been reported to act on STAT3. They are SHP1, SHP2, TC45, and PTPRT (ten Hoeve *et al.* 2002; Yamamoto *et al.* 2002; Zhang *et al.* 2007; Kim *et al.* 2010). SHP2 was shown to act on STAT3 by interacting with phosphorylated Y759 in the gp130 YSTV motif. However, the major PTPase(s) sought should act on STAT3 independently of pY759 of gp130, as shown in Fig. 3C, excluding SHP2 as a candidate. Among the above PTPases, only TC45 is localized mainly to the nucleus in HepG2 cells.

Then, to get insight into the nature of the candidate PTPase, we first examined where the phosphoSer727-dependent dephosphorylation of pY705 STAT3 occurred—in the cytoplasm or the nucleus. We used two types of STAT3 mutants defective for nuclear translocation, an N-terminal deletion mutant of STAT3-162-770 (Liu *et al.* 2005) and a STAT3-K214/215R mutant (Ma *et al.* 2003). These mutants, with either intact S727 or S727A, were expressed in HepG2-stat3KD cells at comparable levels (data not shown). For each type, STAT3-162-770 or STAT3-K214/215R mutants showed dephosphorylation of pY705 at a significantly slower rate than the dephosphorylation of pY705 of STAT3WT, whereas S727A mutants of both STAT3-162-770 and STAT3-K214/215R showed sustained levels of pY705 as STAT3S727A. These data indicate that in contrast to the STAT3 mutants with S727A, STAT3 with the intact S727 lost phosphorylation at Y705 mainly in the nucleus and to a lesser extent in the cytoplasm. Considering that activated STAT3WT mostly translocates to the nuclei, it is likely that phospho-Ser727-dependent dephosphorylation of pY705 may be mainly regulated in the nucleus. Thus, PTPase in the nucleus is likely to be responsible for the dephosphorylation of pY705 in a phospho-Ser727-dependent manner. However, the possibility of some contribution of phosphatase(s) outside the nucleus should be kept in mind, considering that STAT3 itself may shuttle between cytoplasm and nucleus (Liu *et al.* 2005). Because TC45 was mainly localized to the nucleus in HepG2 cells (data not shown), we examined how much TC45 contributed to the dephosphorylation of STAT3 at Y705 in a phospho-Ser727-dependent manner. To evaluate the role of TC45, we knocked down TC45 in both HepG2-STAT3WT and HepG2-STAT3S727A cells using a lentiviral expression system for TC45 shRNA (Fig. 4B). These cells were stimulated with IL-6 for the indicated times, and the STAT3 Y705 phosphorylation was monitored (Fig. 4C). The TC45 knockdown (TC45KD) extended the duration of the pY705 level in STAT3WT, compared with the results shown in Fig. 2D, whereas TC45KD did not alter the rate of pY705 dephosphorylation in STAT3S727A, indicating that TC45 greatly affected the pY705 level of STAT3 with the intact Ser727. It should be noted that the time points used for STAT3S727A cover a longer time frame than that for STAT3WT. To further test the role of TC45, we overexpressed 3×FLAG-TC45 in HepG2-STAT3WT cells and HepG2-STAT3S727A cells. The expression levels of TC45 were approximately
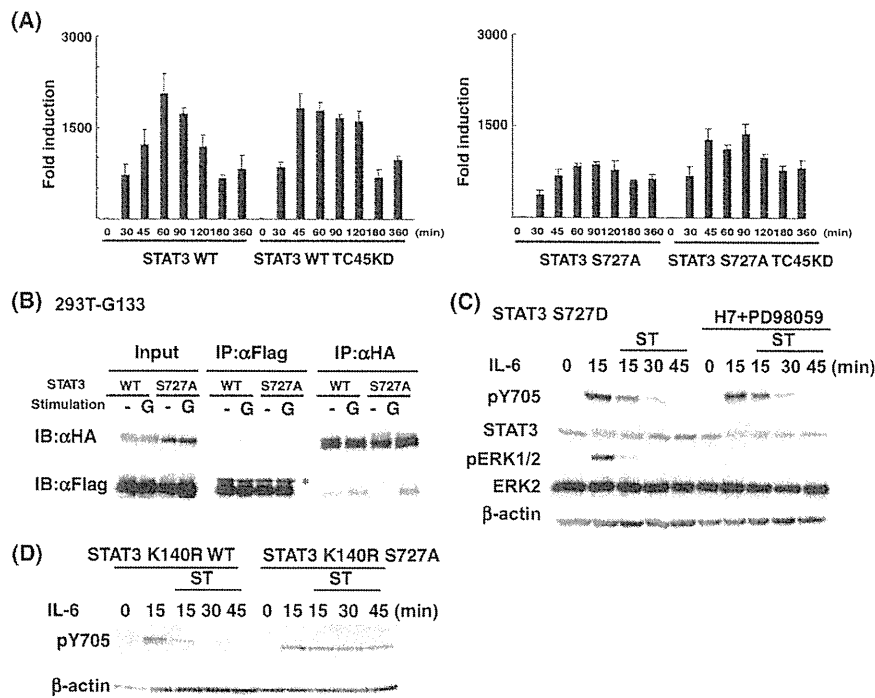
Figure 5 TC45 on STAT3 pY705 needs a post-phospho-Ser727 event(s) to function. (A) HepG2-STAT3WT and HepG2-STAT3WT-TC45KD (left panel), HepG2-STAT3S727A, and HepG2-STAT3S727SA-TC45KD (right panel) cells were stimulated with 20 ng/mL IL-6 for the indicated times. The *socs3* mRNA expression levels in total RNA from each sample were measured by qRT-PCR as in Fig. 1B. The data are averages of three independent experiments; error bars are the standard deviations. (B) 293T-G133 cells were transiently transfected with either HA-tagged STAT3WT or HA-STAT3S727A together with a 3×FLAG-tagged TC45-DA/CS mutant (Asp182 to Ala, Cys216 to Ser). Transfected cells were unstimulated (−) or stimulated with G-CSF at 50 ng/mL for 15 min (G). Whole-cell extracts were immunoprecipitated with anti-FLAG or anti-HA antibodies. Immuno-precipitates were analyzed by immunoblotting using anti-HA and anti-Flag Abs. An asterisk (*) shows a nonspecific protein. (C) HepG2-STAT3S727D cells were pretreated with or without H7 (100 μM) and PD98059 (50 μM) for 30 min then stimulated with IL-6 at 20 ng/mL for 15 min, and treated with staurosporine (ST) (0.5 μM) for the indicated times. Immunoblot analysis was carried out on whole-cell extracts (30 μg per lane) using indicated antibodies. (D) HepG2-STAT3Lys140Arg(K140R)/WT and STAT3K140R/S727A were stimulated with IL-6 (20 ng/mL) for 15 min, and treated with ST (0.5 μM) for the indicated times, then pY705 levels were monitored by immunoblotting.

eight times that of endogenous TC45 mRNA (Fig. 4E). Overexpressed TC45 reduced the overall levels of pY705 of both STAT3WT and STAT3S727A, probably due to the effect on the activity of JAK kinases (Simoncic *et al.* 2002). However, overexpressed TC45 shortened the duration of pY705 of STAT3WT but not that of STAT3S727A (Fig. 4F). This was also the case for the dephosphorylation process analyzed by the use of ST (Fig. 4G). Overexpressed TC45 caused rapid dephosphorylation of pY705 of STAT3WT but did not alter the dephosphorylation rate of pY705 of STAT3S727A. Consistent with this, the inhibition of phospho-Ser727 by the kinase inhibitors, shown in Fig. 3C, also reduced the rate of pY705 dephosphorylation even in the presence of overexpressed TC45 (data not shown).

Unidentified event(s) because of phospho-Ser727 may affect the function of TC45 on STAT3 pY705

To further support the notion that TC45 functions in dephosphorylation of pY705 in a phospho-Ser727-dependent manner, we examined the effect of a TC45 knockdown on STAT3-dependent *socs3* mRNA expression (Fig. 5A). TC45KD caused more sustained *socs3* mRNA expression in STAT3WT cells but not in STAT3S727A cells. Slightly higher *socs3* mRNA expression was observed throughout the tested period in STAT3S727A cells. This may result from the regulation of JAKs activity by TC45 (Simoncic *et al.* 2002). All of the data shown above indicate that TC45 is largely responsible for the dephosphorylation of STAT3 pY705 in a phospho-Ser727-dependent manner.

We next addressed how phospho-Ser727 of STAT3 affected the function of TC45. We then tested whether phospho-Ser727 was required for the interaction between STAT3 and TC45. For this purpose, we used a TC45 mutant, TC45-DA/CS that lacked the phosphatase activity as often used to see the interaction between certain tyrosine phosphatases and their substrates (Tiganis et al. 1999; Tonks et al. 2004). We transiently expressed HA-tagged STAT3WT or HA-STAT3S727A together with 3×FLAG-tagged TC45-DA/CS in 293T-G133 cells expressing the GCSF-R-gp130 chimeric receptor containing a truncated gp130 with cytoplasmic 133 amino acid residues with both a YSTV motif and a YRHQ motif, G133 (Abe et al. 2001). As shown in Fig. 5B, the anti-FLAG antibody immunoprecipitated TC45-DA/CS together with small amounts of HA-STAT3WT or HA-STAT3S727A even in the absence of receptor stimulation, though gp130 stimulation increased the interaction between TC45 and HA-STAT3WT or HA-STAT3S727A. Consistently, immunoprecipitated complexes of HA-STAT3WT or HA-STAT3S727A contained FLAG-TC45-DA/CS, especially after gp130 stimulation. Thus, TC45 interacts with STAT3 independently of phospho-Ser727, suggesting the presence of unidentified and phospho-Ser727-dependent mechanism(s) that allow TC45 to function well.

To gain insight into the events after Ser727 phosphorylation that affect the TC45 function, we tested whether the kinase activities sensitive to H7+PD98059 play a role in regulating pY705 of STAT3S727D. Pretreatment of HepG2-STAT3S727D with H7+ PD98059 did not inhibit the dephosphorylation of pY705 (Fig. 5C). Importantly, the slight changes in STAT3S727D mobility after IL-6 stimulation were observed even in the presence of H7+PD98059 (Fig. 5C). Together with the results shown in Fig. 3D, this result indicates that the kinase activities sensitive to H7+PD98059 in IL-6 signals are involved in Ser727 phosphorylation but not in the post-phospho-Ser727 events causing a further mobility shift nor in enhancing the pY705 dephosphorylation process. In relation to this matter, recently, Yang et al. (2010) showed that dimethylation of STAT3 at K140 by SET9 after Ser727 phosphorylation in the nucleus inhibits STAT3 activity by suppressing the level of pY705 of STAT3. Therefore, we tested whether STAT3K140R mutants defective for being methylated might lose the phospho-Ser727-dependent regulation of pY705 in our system. We expressed both STAT3K140R/WT and STAT3K140R/S727A at a comparable level in HepG2-stat3KD cells (data not shown). As shown in

Fig. 5D, STAT3K140R/WT showed rapid dephosphorylation of pY705 under the tyrosine-kinase inhibition, whereas STAT3-K140R/S727A showed very slow dephosphorylation of pY705. This result excluded the role of a K140 modification in the phospho-Ser727-dependent pY705 dephosphorylation in our HepG2-STAT3 reconstitution system. These data suggest that phospho-Ser727 is functionally required for the dephosphorylation of pY705 largely by TC45 through possibly recruiting a regulatory molecule(s) targeting to phospho-Ser727 or to another region modified in a phospho-Ser727-dependent manner that is distinct from K140 methylation.

Discussion

In this study, we first showed that the intact Ser727 of STAT3 is required for both the maximal transcription of the socs3 gene, one of the STAT3 target genes, and the restricted duration of its mRNA expression from the mechanism intrinsic to the state of STAT3. We showed that this regulated duration of STAT3 action at least partly resulted from phosphorylation at Ser727 by using a combination of the HepG2-stat3KD reconstituted with various STAT3 mutants and the kinase inhibitors, H7 and PD98059, that interfere with phosphorylation of Ser727 in IL-6 signals. This dual role for phospho-Ser727 of STAT3 might be physiologically important to give proper responses with regulated strength and duration of STAT3 activity. The effect of phospho-Ser727 of STAT3 on the regulated gene expression was also observed in other STAT3-inducible genes, including tis11/TTP and acute phase reactants, saa1 and saa2 (unpublished data). ST was used in this study to efficiently inhibit further phosphorylation of Y705 by tyrosine kinases in IL-6/gp130 signals. We should mention the possibility that this reagent might inhibit the kinase activities of some serine/threonine kinases involved in the pathways leading to phospho-Ser727 in this receptor system. However, considering the fact that phospho-Ser727 of STAT3 remained well after the rapid decrease of pY705 in STAT3 WT after the treatment with ST (Fig. 3D), we believe that the role of phospho-Ser727 in the rapid dephosphorylation of Y705 was properly evaluated in this study.

Multiple PTPases including SHP2, SHP1, TC45, and PTP-RT (ten Hoeve et al. 2002; Yamamoto et al. 2002; Zhang et al. 2007; Kim et al. 2010) have been shown to regulate STAT3 activity. Among these PTPases, we have shown that TC45 is likely a major PTPase for the phospho-Ser727-dependent pY705

dephosphorylation from the following layers of supporting evidence: (i) phospho-Ser727-dependent dephosphorylation is likely to occur mainly in the nucleus, as judged by the reduced rate of pY705 dephosphorylation in two STAT3 mutants devoid of nuclear translocation, (ii) TC45-knockdown affected the pY705 duration as well as the duration of *socs3* mRNA expression in HepG2-STAT3WT cells but not in HepG2-STAT3S727A cells, (iii) overexpression of TC45 again affected the pY705 dephosphorylation of STAT3WT but not that of STAT3S727A. However, at least one cytoplasmic or membrane phosphatase distinct from TC45 may need the intact Ser727 or phosphorylated Ser727 to function, based on the results that S727A in the STAT3 mutants devoid of nuclear translocation also showed sustained pY705 (Fig. 4A). Considering that when cells were stimulated with the YXXQ signal alone instead of IL-6, both STAT3WT and STAT3S727A showed a higher dephosphorylation rate (Fig. 3C), there must be another tyrosine phosphatase that dephosphorylates pY705 independently of phospho-Ser727 under the pYXXQ-derived signals. Thus, STAT3 inactivation through tyrosine dephosphorylation is regulated by multiple mechanisms involving multiple PTPases and multiple signals.

Interestingly, the interaction of TC45 with STAT3 did not require phospho-Ser727. This suggests that the action of TC45 on pY705 of STAT3 is regulated not only by the interaction between them but also by some unidentified mechanism(s) that occurs in a phospho-Ser727-dependent manner. Such mechanisms seem to use a regulatory molecule(s) targeting a region including phospho-Ser727 or another STAT3 region modified in a phospho-Ser727-dependent manner. The possible STAT3 modifications involved in such regulation may include phosphorylation, acetylation, methylation, sumoylation, ubiquitilation, and other unidentified modifications. Yang *et al.* (2010) recently showed that activated STAT3 was methylated on K140 by the histone methyltransferase SET9 in the nucleus after Ser727 phosphorylation and that the methylation of STAT3 had negative regulatory effects on pY705 and STAT3-dependent transcription of some genes, including the *socs3* gene. However, we found that STAT3-K140 methylation did not account for the phospho-Ser727-dependent dephosphorylation of Y705 in our system. STAT3 has been shown to be acetylated at K685 (Wang *et al.* 2005; Yuan *et al.* 2005), K49 and K87 (Ray *et al.* 2005), and K679, K685, K707, and K709 (Nie *et al.* 2009). There was one report showing a relationship between

STAT3 acetylation and phosphotyrosine levels. Nie *et al.* (2009) showed that SirT1 negatively regulates STAT3 phosphotyrosine level by deacetylating the multiply acetylated STAT3. Based on their data, it is likely that acetylation of STAT3 at multiple lysines in the carboxy-terminus, K679, K685, K707, and K709, protects activated STAT3 from PTPase action. Thus, such acetylation of STAT3 causes sustained activation of STAT3, making it unlikely for the acetylation of STAT3 on these sites to be involved in the negative regulation shown in this study. We have seen mobility shifts of STAT3WT but not of STAT3S727A after IL-6 stimulation or stimulation of gp130-YXXQ-derived signals, as shown in Fig. 3A,C,D. These mobility shifts most likely result from phosphorylation of multiple sites in addition to Ser727. As the STAT3S727A mutant does not show apparent mobility shifts, such phosphorylation events, if any, should be dependent on phospho-Ser727. This is also supported by the result showing that STAT3S727D itself caused a slight mobility shift but that STAT3S727D showed a further small mobility shift after stimulation (Fig. 5C). Because the contribution of pY705 in the mobility shifts seemed to be negligible, as shown Fig. 3A, in addition to the phosphorylation of Y705, STAT3S727D is likely to undergo a further modification that results in the further mobility shift. Interestingly, the modification event observed in IL-6-stimulated STAT3S727D was resistant to the treatment with H7+PD98059. Considering that dephosphorylation of pY705 of STAT3S727D is also resistant to the kinase inhibitors, the unidentified events affecting the mobility shift because of phospho-Ser727, or S727D, might be involved in regulating the activity of PTPases including TC45. Identification of modification event(s) and the amino acid residues receiving such modification is needed to clarify the mechanism.

The roles of phospho-Ser727 of STAT3 in the gene transcription have been reported since the discovery of the phosphorylation of Ser727, in addition to the critical tyrosine phosphorylation (Wen *et al.* 1995). Most studies relied on the use of the STAT3 mutants, STAT3S727A and STAT3S727D (Wen & Darnell 1997; Abe *et al.* 2001; Shen *et al.* 2004), used in this study. The use of such mutants may reduce the validity of deductions about the role of phospho-Ser727 in some cases. Sun *et al.* (2006) showed that the conserved LPMSP motif around Ser727 itself is required for p300 recruitment by STAT3 to the target gene regulatory regions. They showed that some mutations introduced at the motif disrupt the proper

recruitment of p300 without hampering the phosphorylation of Ser727, although their findings do not exclude the role of phospho-Ser727 in the regulation of STAT3-dependent gene transcription. In our preliminary experiments, HepG2-STAT3S727D cells induced a *socs3* mRNA expression of short duration, consistent with the role of phospho-Ser727 in enhancing dephosphorylation of pY705 (unpublished data). Studies of the regulatory mechanisms by which IL-6 activates transcription of STAT3 target genes, including the roles of phospho-Ser727, are currently underway. The study of the role of phospho-Ser727 of STAT3 in gene regulation apparently requires more sophisticated methods.

Although we report that the role of phospho-Ser727 in IL-6 signals negatively regulates the duration of STAT3 activity by enhancing dephosphorylation of pY705 largely through TC45, the same mechanism may inhibit STAT3 activity when phosphorylation of Ser727 precedes Y705 tyrosine phosphorylation in the cases of the combined stimulation of cells with some factors causing phospho-Ser727 and some causing pY705 of STAT3, or under some conditions in which cells have both active serine/threonine kinases for Ser727 and tyrosine kinases for Tyr705 of STAT3. Actually, such cases or conditions have been reported. Andersson *et al.* (2007) showed that insulin inhibits IL-6-induced STAT3 activity through SHP-2 and MEK/ERK1/2-dependent pathways. They showed that insulin enhanced phospho-Ser727 but reduced phospho-Tyr705 of STAT3 when given together with IL-6 and that the inhibitory effect of insulin was mostly reversed with PD98059 treatment. Shi *et al.* (2006) found that the enhanced level of STAT3 Ser727 phosphorylation during mitosis, which was shown to be induced by cyclin-dependent kinase 1, correlated well with a reduction of Y705 phosphorylation of STAT3 and that the reduction of STAT3 activity during mitosis was likely to be involved in the regulation of the cell cycle. These two reports discussed the negative relationship between phospho-Ser727 and phospho-Tyr705 of STAT3. Our findings on the role of phosphorylation of Ser727 in negatively regulating pY705 largely through TC45 may explain the underlying mechanism of their results.

STAT3 activation has been shown to be critical in the development of certain types of tumors (Bowman *et al.* 2000; Kim *et al.* 2007). In the many instances of such *in vivo* tumor cells, both phospho-Y705 and phospho-S727 have been often observed. In those cells, phospho-S727 in STAT3 has been argued to have positive roles in STAT3 function (Lee *et al.*

2009). It is possible that some mechanisms negating the negative role of phospho-Ser727 may be present in some tumor cells utilizing STAT3 as a transcription factor causing survival and proliferative signals.

Our study provides evidence showing that phospho-Ser727 enhances dephosphorylation of pY705 of STAT3 largely through TC45, and implies the existence of an unidentified post-phospho-Ser727 process for the efficient function of TC45. Thus, in-depth understanding of the molecular mechanisms following phospho-Ser727 will shed light on the mechanisms determining the overall roles of phospho-Ser727, both negative and positive, in STAT3 functions in different settings.

Experimental procedures

Reagents and antibodies

Recombinant human IL-6 was a gift from Ajinomoto Research Institute (Tokyo, Japan). Recombinant human G-CSF was purchased from Kyowa Hakko Kirin Co., Ltd. (Tokyo, Japan). Antibodies (Abs) to STAT3, RNA polymerase II (Pol II), β-actin, ERK1/2, and phospho-ERK1/2 were from Santa Cruz Biotechnology (Santa Cruz, CA, USA). Abs to phospho-STAT3 (Tyr705) and phospho-STAT3 (Ser727) were from Cell Signaling Technology (Beverly, MA, USA). The anti-FLAG monoclonal Ab (M2) was from Sigma-Aldrich (Saint Louis, MO, USA), and anti-HA Ab was from Roche Diagnostics (Indianapolis, IN, USA). 1-(5-Iso-quinolinylsulfo-nyl)-2-methylpiperazine (H7) was from Sigma-Aldrich. MEK inhibitor PD98059 was from Calbiochem (La Jolla, CA, USA). All other reagents purchased from Nacalai Tesque Inc. (Kyoto, Japan).

Plasmids and siRNA

The siRNA-resistant STAT3WT was described previously (Zhao *et al.* 2004). All of the STAT3 mutants, STAT3S727A (Ser727 to Ala), STAT3S727D (Ser727 to Asp), STAT3K214R/K215R/WT (Lys214 to Arg, Lys215 to Arg), STAT3K214R/K215R/S727A, STAT3K140R/WT (Lys140 to Arg), and STAT3K140R/S727A were made using the quick-change mutation system (Stratagene, La Jolla, CA, USA). Two STAT3 N-terminal deletion mutants, STAT3-162-770/WT and STAT3-162-770/S727A, were produced by PCR. Sequences of all of the mutants were verified by DNA sequencing. Each Stat3 cDNA was transferred into a lentiviral vector, pCSII-EF-MCS-IRES-Venus (a gift from H. Miyoshi, RIKEN, Tsukuba, Japan). To generate the pCSII-EF-3xFlagTC45, the entire coding region was amplified by PCR using pCMV-SPORT6-TC45 (Clone ID 3872164) purchased from OpenBiosytems (Huntsville, AL, USA) as a template and the resulting cDNA with the *Eco*RI and *Bam*HI

sites at both ends was cloned into pCSII-EF-3xFLAG-IRES-Venus at the *Eco*RI/*Bam*HI site. The TC45DA/CS (Asp182 to Ala, Cys216 to Ser) mutant was made using the quick-change mutation system. To make TC45 knockdown cells, we used a lentiviral miRNA-type shRNA expression system. The oligonucleotide for the shRNA against human TC45 was as follows: TC45-mishRNA-1077: TGCTGAAAGGCAGGAGA TAAGTCTTCGTTTTGGCCACTGACTGACGAAGACTT CTCCTGCCTTT.

Cell lines

All HepG2 cell lines were grown in DMEM supplemented with 10% FCS (GIBCO, Grand Island, NY, USA), and HEK293T cells were grown with 5% FCS. The HepG2 cell line with stat3 mRNA knockdown (HepG2-stat3KD) was used for reconstitution of mutated STAT3 (Zhao *et al.* 2004). Lentiviral preparations expressing STAT3 mutants were produced as described previously and infected into HepG2-stat3KD cells.

Immunoblotting and immunoprecipitation

The cells were washed twice with ice-cold phosphate-buffered saline and then lysed with whole-cell extract buffer (20 mM Hepes, pH 7.9, 1% NP-40, 400 mM NaCl, 20% glycerol, 10 mM NaF, 1 mM PMSF, 1 mM sodium vanadate, 1 mM EDTA, 1 mM EGTA, 1 µg/mL leupeptin, 1 µg/mL pepstatin, and 1 µg/mL aprotinin). The cell lysates were centrifuged at 14 000 g for 10 min at 4 °C, and the resulting supernatants were used. Immunoprecipitation analysis was carried out as described previously (Kojima *et al.* 2005). Whole cell extracts or immunoprecipitates were separated by 7.5% SDS–PAGE, transferred onto polyvinylidene difluoride (PVDF) membranes, and probed with the indicated antibodies. Signals were detected with Chemi-Lumi One (Nacalai Tesque).

Quantitative real-time PCR

RNA was isolated with Sepasol RNA I super (Nacalai Tesque) and treated with RQ1 RNase-free DNase I (Promega, Madison, WI, USA). Reverse transcriptase reaction for cDNA synthesis was made using a ReverTra Ace qPCR RT kit (Toyobo Co Ltd., Osaka, Japan). Relative quantification was carried out using the ABI 7500 Fast System (Applied Biosystems). Primers were designed using PRIMER EXPRESS software (Applied Biosystems), and sequences are as below. Relative quantities of target transcripts were calculated from duplicate samples after normalization of the data against the endogenous control, hGAPDH-Forward; 5′-GCACCGTCAA GGCTGAGAAC-3′, hGAPDH-Reverse; 5′-TGGTGAAGAC GCCAGTGGA-3′, hSOCS3-Forward; 5′-GGAATGTAGCA GCGATGGAA-3′, hSOCS3-Reverse; 5′-GCCCTGTCCAGC CCAATAC-3′, hGCSFRgp108YRHQ-Forward; 5′-CTCTCC TGCCTCATGAACCTC-3′, hGCSFRgp108YRHQ-Reverse; 5′-GTGAAGCTGGTGGGTAGGTG-3′, hSTAT3-Forward;

5′-ACTCCATCCTGGGCGACAGT-3′, hSTAT3-Reverse; 5′-TTGACCTGAAGCCCGTTTC-3′, hTC45-Forward; 5′-TT TTGGAGTCCCTGAATCACC-3′, hTC45-Reverse; 5′-GCC CAATGCCTGCACTACA-3′.

Chromatin immunoprecipitation assays

Chromatin immunoprecipitation (ChIP) was carried out according to the manufacturer's instructions (Upstate Biotechnology, Lake Placid, NY, USA). Briefly, the HepG2-derivative cell lines were stimulated with IL-6 at 20 ng/mL for the indicated times, and the cells were fixed with 1% formaldehyde (final concentration) for 10 min at 37 °C, lysed, and sonicated. Immunoprecipitates with specific antibodies were incubated with proteinase K overnight at 65 °C, and then the DNA fragments included in the immunoprecipitates were purified. PCR was carried out using the ABI 7500 Fast System (Applied Biosystems, Foster City, CA, USA). The primer sets were the following: the human SOCS3 promoter region (−115 to −49), Forward 5′-TTTCTCTGCTGCGAG TAGTGACTAA-3′, Reverse 5′-CCCCCGATTCCTGGA ACT-3′ and the 3′ end of the SOCS3 gene (2899 to 3024), Forward 5′-GGAATGTAGCAGCGATGGAA-3′, Reverse 5′-GCCCTGTCCAGCCCAATAC-3′.

References

Abe, K., Hirai, M., Mizuno, K., Higashi, N., Sekimoto, T., Miki, T., Hirano, T. & Nakajima, K. (2001) The YXXQ motif in gp130 is crucial for STAT3 phosphorylation at Ser727 through an H7-sensitive kinase pathway. *Oncogene* **20**, 3464–3474.

Andersson, C.X., Sopasakis, V.R., Wallerstedt, E. & Smith, U. (2007) Insulin antagonizes interleukin-6 signaling and is anti-inflammatory in 3T3-L1 adipocytes. *J. Biol. Chem.* **282**, 9430–9435.

Boulton, T.G., Zhong, Z., Wen, Z., Darnell, J.E., Stahl, N. & Yancopoulos, G.D. (1995) STAT3 activation by cytokines utilizing gp130 and related transducers involves a secondary modification requiring an H7-sensitive kinase. *Proc. Natl Acad. Sci. USA* **92**, 6915–6919.

Bowman, T., Garcia, R., Turkson, J. & Jove, R. (2000) STATs in oncogenesis. *Oncogene* **19**, 2474–2488.

Chung, J., Uchida, E., Grammer, T.C. & Blenis, J. (1997) STAT3 serine phosphorylation by ERK-dependent and

-independent pathways negatively modulates its tyrosine phosphorylation. *Mol. Cell. Biol.* **17**, 6508–6516.

Darnell, J.E. Jr (1997) STATs and gene regulation. *Science* **277**, 1630–1635.

Darnell, J.E. Jr, Kerr, I.M. & Stark, G.R. (1994) Jak-STAT pathways and transcriptional activation in response to IFNs and other extracellular signaling proteins. *Science* **264**, 1415–1421.

Decker, T. & Kovarik, P. (2000) Serine phosphorylation of STATs. *Oncogene* **19**, 2628–2637.

Fu, A.K., Fu, W.Y., Ng, A.K., Chien, W.W., Ng, Y.P., Wang, J.H. & Ip, N.Y. (2004) Cyclin-dependent kinase 5 phosphorylates signal transducer and activator of transcription 3 and regulates its transcriptional activity. *Proc. Natl Acad. Sci. USA* **101**, 6728–6733.

Fukada, T., Hibi, M., Yamanaka, Y., Takahashi-Tezuka, M., Fujitani, Y., Yamaguchi, T., Nakajima, K. & Hirano, T. (1996) Two signals are necessary foe cell proliferation induced by a cytokine receptor gp130: involvement of STAT3 in anti-apoptosis. *Immunity* **5**, 449–460.

Haspel, R.L. & Darnell, J.E. (1999) A nuclear protein tyrosine phosphatase is required for the inactivation of Stat1. *Proc. Natl Acad. Sci. USA* **96**, 10188–10193.

Hirano, T., Nakajima, K. & Hibi, M. (1999) Signaling mechanisms through gp130: a model of the cytokine system. *Cytokine Growth Factor Rev.* **8**, 241–252.

ten Hoeve, J., de Jesus Ibarra-Sanchez, M., Fu, Y., Zhu, W., Tremblay, M., David, M. & Shuai, K. (2002) Identification of a nuclear Stat1 protein tyrosine phosphatase. *Mol. Cell. Biol.* **22**, 5662–5668.

Jain, N., Zhang, T., Kee, W.H., Li, W. & Cao, X. (1999) Protein kinase C delta associates with and phosphorylates Stat3 in an interleukin-6-dependent manner. *J. Biol. Chem.* **274**, 24392–24400.

Kim, D.J., Chan, K.S., Sano, S. & DiGiovanni, J. (2007) Signal transducer and activator of transcription 3 (Stat3) in epithelial carcinogenesis. *Mol. Carcinog.* **46**, 725–731.

Kim, D.J., Tremblay, M.L. & DiGiovanni, J. (2010) Protein tyrosine phosphatases, TC-PTP, SHP1, and SHP2, cooperate in rapid dephosphorylation of Stat3 in keratinocytes following UVB irradiation. *PLoS ONE* **5**, e10290.

Kojima, H., Sasaki, T., Ishitani, T., Iemura, S., Zhao, H., Kaneko, S., Kunimoto, H., Natsume, T., Matsumoto, K. & Nakajima, K. (2005) STAT3 regulates Nemo-like kinase by mediating its interaction with IL-6-stimulated TGFbeta-activated kinase 1 for STAT3 Ser-727 phosphorylation. *Proc. Natl Acad. Sci. USA* **102**, 4524–4529.

Lee, H., Herrmann, A., Deng, J.H., Kujawski, M., Niu, G., Li, Z., Forman, S., Jove, R., Pardoll, D.M. & Yu, H. (2009) Persistently activated Stat3 maintains constitutive NF-kappaB activity in tumors. *Cancer Cell* **15**, 283–293.

Lehmann, U., Schmitz, J., Weissenbach, M., Sobota, R.M., Hortner, M., Friederichs, K., Behrmann, I., Tsiaris, W., Sasaki, A., Schneider-Mergener, J., Yoshimura, A., Neel, B.G., Heinrich, P.C. & Schaper, F. (2003) SHP2 and SOCS3 contribute to Tyr-759-dependent attenuation of interleukin-6 signaling through gp130. *J. Biol. Chem.* **278**, 661–671.

Levy, D.E. & Darnell, J.E. (2002) Stats: transcriptional control and biological impact. *Nat. Rev. Mol. Cell Biol.* **3**, 651–662.

Li, W., Nishimura, R., Kashishian, A., Batzer, A.G., Kim, W.J.H., Cooper, J.A. & Schlessinger, J. (1994) A new function for a phosphotyrosine phosphatase: linking GRB2-Sos to a receptor tyrosine kinase. *Mol. Cell. Biol.* **14**, 509–517.

Liu, L., McBride, K.M. & Reich, N.C. (2005) STAT3 nuclear import is independent of tyrosine phosphorylation and mediated by importin-alpha3. *Proc. Natl Acad. Sci. USA* **102**, 8150–8155.

Lufei, C., Koh, T.H., Uchida, T. & Cao, X. (2007) Pin1 is required for the Ser727 phosphorylation-dependent Stat3 activity. *Oncogene* **26**, 7656–7664.

Ma, J., Zhang, T., Novotny-Diermayr, V., Tan, A.L.C. & Cao, X. (2003) A novel sequence in the coiled-coil domain of Stat3 essential for its nuclear translocation. *J. Biol. Chem.* **278**, 29252–29260.

Mertens, C. & Darnell, J.E. (2007) SnapShot: JAK-STAT signaling. *Cell* **131**, 612.

Nicholson, S.E., Willson, T.A., Farley, A., Starr, R., Zhang, J.G., Baca, M., Alexander, W.S., Metcalf, D., Hilton, D.J. & Nicola, N.A. (1999) Mutational analyses of the SOCS proteins suggest a dual domain requirement but distinct mechanisms for inhibition of LIF and IL-6 signal transduction. *EMBO J.* **18**, 375–385.

Nie, Y., Erion, D.M., Yuan, Z., Dietrich, M., Shulman, G.I., Horvath, T.L. & Gao, Q. (2009) STAT3 inhibition of gluconeogenesis is downregulated by SirT1. *Nat. Cell Biol.* **11**, 492–500.

Ohkawara, B., Shirakabe, K., Hyodo-Miura, J., Matsuo, R., Ueno, N., Matsumoto, K. & Shibuya, H. (2004) Role of the TAK1-NLK-STAT3 pathway in TGF-beta-mediated mesoderm induction. *Genes Dev.* **18**, 381–386.

Ray, S., Boldogh, I. & Brasier, A.R. (2005) STAT3 NH2-terminal acetylation is activated by the hepatic acute-phase response and required for IL-6 induction of angiotensinogen. *Gastroenterology* **129**, 1616–1632.

Sato, N., Kawai, T., Sugiyama, K., Muromoto, R., Imoto, S., Sekine, Y., Ishida, M., Akira, S. & Matsuda, T. (2005) Physical and functional interactions between STAT3 and ZIP kinase. *Int. Immunol.* **17**, 1543–1552.

Schmitz, J., Dahmen, H., Grimm, C., Gendo, C., Müller-Newen, G., Heinrich, P.C. & Schaper, F. (2000) The cytoplasmic tyrosine motifs in full-length glycoprotein 130 have different roles in IL-6 signal transduction. *J. Immunol.* **164**, 848–854.

Schuringa, J.J., Schepers, H., Vellenga, E. & Kruijer, W. (2001) Ser727-dependent transcriptional activation by association of p300 with STAT3 upon IL-6 stimulation. *FEBS Lett.* **495**, 71–76.

Shen, Y., Schlessinger, K., Zhu, X., Meffre, E., Quimby, F., Levy, D.E. & Darnell, J.E. Jr (2004) Essential role of STAT3 in postnatal survival and growth revealed by mice

lacking STAT3 serine 727 phosphorylation. *Mol. Cell. Biol.* **24**, 407–419.

Shi, X., Zhang, H., Paddon, H., Lee, G., Cao, X. & Pelech, S. (2006) Phosphorylation of STAT3 serine-727 by cyclin-dependent kinase 1 is critical for nocodazole-induced mitotic arrest. *Biochemistry* **45**, 5857–5867.

Simoncic, P.D., Lee-Loy, A., Barber, D.L., Tremblay, M.L. & McGlade, C.J. (2002) The T cell protein tyrosine phosphatase is a negative regulator of janus family kinases 1 and 3. *Curr. Biol.* **12**, 446–453.

Stahl, N., Farruggella, T.J., Boulton, T.G., Zhong, Z., Darnell, J.E. Jr & Yancopoulos, G.D. (1995) Choice of STATs and other substrates specified by modular tyrosine-based motifs in cytokine receptors. *Science* **267**, 1349–1352.

Sun, W., Snyder, M., Levy, D.E. & Zhang, J.J. (2006) Regulation of Stat3 transcriptional activity by the conserved LPMSP motif for OSM and IL-6 signaling. *FEBS Lett.* **580**, 5880–5884.

Terstegen, L., Gatsios, P., Bode, J.G., Schaper, F., Heinrich, P.C. & Graeve, L. (2000) The inhibition of interleukin-6-dependent STAT activation by mitogen-activated protein kinases depends on tyrosine 759 in the cytoplasmic tail of glycoprotein 130. *J. Biol. Chem.* **275**, 18810–18817.

Tiganis, T., Kemp, B.E. & Tonks, N.K. (1999) The protein-tyrosine phosphatase TCPTP regulates epidermal growth factor receptor-mediated and phosphatidylinositol 3-kinase-dependent signaling. *J. Biol. Chem.* **274**, 27768–27775.

Tonks, N.K., Meng, T.C., Buckley, D.A., Galic, S. & Tiganis, T. (2004) Regulation of insulin signaling through reversible oxidation of the protein-tyrosine phosphatases TC45 and PTP1B. *J. Biol. Chem.* **279**, 37716–37725.

Wang, R., Cherukuri, P. & Luo, J. (2005) Activation of Stat3 sequence-specific DNA binding and transcription by p300/CREB-binding protein-mediated acetylation. *J. Biol. Chem.* **280**, 11528–11534.

Wen, Z. & Darnell, J.E. (1997) Mapping of Stat3 serine phosphorylation to a single residue (727) and evidence that serine phosphorylation has no influence on DNA binding of Stat1 and Stat3. *Nucleic Acids Res.* **25**, 2062–2067.

Wen, Z., Zhong, Z. & Darnell, J.E. (1995) Maximal activation of transcription by Stat1 and Stat3 requires both tyrosine and serine phosphorylation. *Cell* **82**, 241–250.

Wierenga, A.T., Vogelzang, I., Eggen, B.J. & Vellenga, E. (2003) Erythropoietin-induced serine 727 phosphorylation of STAT3 in erythroid cells is mediated by a MEK-, ERK-, and MSK1-dependent pathway. *Exp. Hematol.* **31**, 398–405.

Yamamoto, T., Sekine, Y., Kashima, K., Kubota, A., Sato, N., Aoki, N. & Matsuda, T. (2002) The nuclear isoform of protein-tyrosine phosphatase TC-PTP regulates interleukin-6-mediated signaling pathway through STAT3 dephosphorylation. *Biochem. Biophys. Res. Commun.* **297**, 811–817.

Yang, J., Huang, J., Dasgupta, M., *et al.* (2010) Reversible methylation of promoter-bound STAT3 by histone-modifying enzymes. *Proc. Natl Acad. Sci. USA* **107**, 21499–21504.

Yokogami, K., Wakisaka, S., Avruch, J. & Reeves, S.A. (2000) Serine phosphorylation and maximal activation of STAT3 during CNTF signaling is mediated by the rapamycin target mTOR. *Curr. Biol.* **10**, 47–50.

Yoshimura, A., Naka, T. & Kubo, M. (2007) SOCS proteins, cytokine signaling and immune regulation. *Nat. Rev. Immunol.* **7**, 453–465.

Yuan, Z.-L., Guan, Y.-J., Chatterjee, D. & Chin, Y.E. (2005) Stat3 dimerization regulated by reversible acetylation of a single lysine residue. *Science* **307**, 269–273.

Zhang, X., Guo, A., Yu, J., Possemato, A., Chen, Y., Zheng, W., Polakiewicz, R.D., Kinzler, K.W., Vogelstein, B., Velculescu, V.E. & Wang, Z.J. (2007) Identification of STAT3 as a substrate of receptor protein tyrosine phosphatase T. *Proc. Natl Acad. Sci. USA* **104**, 4060–4064.

Zhao, H., Nakajima, R., Kunimoto, H., Sasaki, T., Kojima, H. & Nakajima, K. (2004) Region 752-761 of STAT3 is critical for SRC-1 recruitment and Ser727 phosphorylation. *Biochem. Biophys. Res. Commun.* **325**, 541–548.

Supporting Information/supplementary material

The following Supporting Information can be found in the online version of the article:

Figure S1 No apparent effect of MG132 on the levels of STAT3 or phospho-Y705 levels.

Additional Supporting Information may be found in the online version of this article.

Please note: Wiley-Blackwell are not responsible for the content or functionality of any supporting materials supplied by the authors. Any queries (other than missing material) should be directed to the corresponding author for the article.

Review article

Hereditary progressive dystonia with marked diurnal fluctuation

Masaya Segawa *

Segawa Neurological Clinic for Children, 2–8 Surugadai Kanda, Chiyoda-ku, Tokyo 101-0062, Japan

Abstract

Hereditary progressive dystonia with marked diurnal fluctuation (HPD) is a dopa-responsive dystonia, now called autosomal dominant GTP cyclohydrolase 1 deficiency or Segawa disease, caused by mutation of the GCH-1 gene located on 14q22.1 to q22.2. Because of heterozygous mutation, partial deficiency of tetrahydrobiopterin affects tyrosine hydroxylase (TH) rather selectively and causes decrease of TH in the terminals of the nigrostriatal dopamine (NS DA) neurons, projecting to the D1 receptors on the striosome, the striatal direct pathways and the subthalamic nucleus (STN) and the D4 receptors of the tuberoinfundibular tract. The activities of TH in the terminal are high in early childhood decrease exponentially to the stational level around early twenties, and show circadian oscillatron. TH in HPD follows these variations with around 20% of normal levels and with development of the downstream structures show appears characteristic clinical symptoms age dependently.

In late fetus period to early infancy, through the striosome-substantia nigra pars compacta pathway failure in morphogenesis of the DA neurons in substantia nigra, in childhood around 6 years postural dystonia through the D1 direct pathways and the descending output of the basal ganglia. Diurnal fluctuation is apparent in childhood but decrease its grade with age.

TH deficiency at the terminal on the STN causes action dystonia from around 8 years and postural tremor from around 10 years, focal dystonia in adulthood.

Adult onset cases in the family with action dystonia start with writer's cramp, torticollis or generalized rigid hypertonus with tremor but do not show postural dystonia. TH deficiency on the D4 receptors causes stagnation of the body length in childhood. With or without action dystonia depends on the locus of mutation. Postural dystonia is inhibitory disorder, while action dystonia is excitatory disorder. The TH deficiency at the terminal does not cause morphological changes or degenerative process. Thus, levodopa shows favorable effects without any relation to the duration of illness.
© 2010 Published by Elsevier B.V. on behalf of the Japanese Society of Child Neurology.

Keywords: Autosomal dominant GCH-1 deficiency; Segawa disease; Postural type; Action type; Pteridine metabolism

1. Introduction

Hereditary progressive dystonia with marked diurnal fluctuation (HPD) is a dopa-responsive dystonia described by Segawa et al. in 1976 [1]. After discovery of the causative gene, the gene of GTP cyclohydrolase 1 (GCH-1) located on 14q22.1 to q22.2 [2], this is called as autosomal dominant GCH-1 deficiency or Segawa disease. Clinically there are two types, postural dystonia and action dystonia type [3,4]. It depends on the family or the loci of mutation. In postural type the clinical symptoms are similar inter- and intra-families, however, action type shows intra-familial variations.

In this article clinical characteristics, neurophysiological, biochemical, neuroimaging, and neuropathological findings are reviewed. Pathophysiologies of these two types are discussed. Lastly, the pathophysiology of the early onset cases, another phenotype are commented.

* Tel.: +81 3 3294 0371; fax: +81 3 3294 0290.
E-mail address: segawa@segawa-clinic.jp

2. Clinical characteristics

In most cases the symptoms at onset is dystonic posture, with rigidity in one lower extremity, pes equinovarus, around 6 years. Clinical course was clarified by an experience of 51 years female with postural type having clinical course of 43 years after onset at 8 years, that is postural dystonia expands to other limbs, and all limbs and trunk muscles are affected by late teens, the rigidity aggravates progressively until around 20 years of age, but the progression subsides in twenties and becomes stationary in the thirties. Postural tremor with high cycles of 8–10 Hz appears after 10 years in an upper extremity and expands to all limbs by thirties. However, locomotion is preserved throughout the course.

In action dystonia type besides postural dystonia dystonic movements of an upper extremity or action retrocollis appear around 8 years. The latter may associate oculogyric crises. From experiences of 38 years female patients with 30 years clinical course and of a childhood onset case with long term follow up, torticollis and writer's cramp appear in adulthood. In families with action dystonia type, there are adult onset cases who start with writer's cramp, torticollis or generalized rigid hypertonus with postural tremor, but do not show dystonic posture or apparent progression.

Symptoms show marked diurnal fluctuation in childhood. But it attenuates the grade with age and becomes unapparent with cessation of clinical progression. In adult onset cases it is not observed. Childhood onset cases show stagnation of body length with onset of dystonia. This is not observed in cases with onset after adolescence.

A few patients show migraineous headache, autistic features, depressive reaction or obsessive behavior. Patients with onset early in infancy start with delay in motor and psychomental development.

Childhood onset cases show marked female predominance. In our personal cases (41 cases from 20 families) F:M is 33:8, that is 4:1, and it is more marked in postural type 18:1 than action type 2:1. While adult onset cases show male predominance. Furukawa et al. [5] showed higher penetrance (87%) in females than males (38%).

Neurological examinations reveal rigid hypertonus [3,4]. But in contrast to Parkinson disease (PD) it is not plastic rigidity, and cases with tremor do not show cogwheel rigidity. These clinical signs, particularly rigidity and tremor, show asymmetry. Exaggeration of tendon reflexes, some with ankle clonus, are observed in child patients, however Babinski sign is negative. In advanced stage, pulsion is observed but freezing phenomenon is not detected because of preservation of locomotion. Cerebral or cerebellar sings or sensory abnormalities are not observed. Early onset patients show postural or truncal hypotonia, failure in locomotion in infancy, camptocormia in late childhood and parkinsonism in adulthood besides symptoms of HPD.

In child onset cases, a dose of 20 mg/kg/day of plain levodopa (levodopa without decarboxylase inhibitor) or 4–5 mg/kg/day with decarboxylase inhibitor show complete and sustained effects without side effects [3,4,6]. There are families in which plain levodopa is effective throughout the course. However, in other family, replacement to L-dopa with decarboxylase inhibitor is necessary from around 13 years, because of activation of the decarboxylation of dopa in the intestine [6]. In a few cases choreic movements develop by a rapid increase of dosage or by administration of a high dose of levodopa in initial stage of treatment [4]. In these patients by reduction of the dosage and slow titration to the optimal doses, favorable and sustained effect is obtained without unfavorable side-effects [6].

However, for action dystonia and related symptoms effects of levodopa may be incomplete, and action retrocollis and oculogyric crises may be aggravated by initial doses [3,4]. Furthermore, patients with this type may show levodopa induced dyskinesia.

The short stature caused by stagnation of the body length recovers completely, if levodopa is administered before adolescent.

Anticholinergics showed a marked and sustained effect for dystonia, but not for tremor [3]. Moderate effects of tetrahydrobiopterin (BH$_4$) with levodopa were reported, but no favorable effects with monotherapy [3].

Before the era of L-dopa stereotactic operations were performed on two patients, one patient with postural type dystonia [7] and the other with action type reported as juvenile parkinsonism [8] whose GCH-1 mutations were identified later [7,8]. Pallidotomy showed moderate effects on postural dystonia but not on tremor [7]. Ventrolateral thalamotomy was effective on tremor [7], rigidity and levodopa induced dyskinesia occurring in adult with action type [8], but no effect on postural dystonia [7].

The age related clinical course observed in a case with long clinical course is explained by following the age variation of the activities of tyrosine hydroxylase (TH) in the synaptic terminals of the caudate nucleus of the nigrostriatal (NS) DA neurons shown by McGeer and McGeer [9] with low levels of TH (Fig. 1). TH activities of the NS DA neurons do now show the state dependent variation in the SNc while show circadian oscillation in the terminals [9]. These evidences implicated that HPD is caused by non-progressive decrease of TH activities in the terminals of the NS DA neuron and develops clinical symptoms following the age and circadian variation of the TH activities of the terminals.

3. Studies for evaluation of the pathophysiology

Polysomnographies (PSGs) performed to clarify the sleep effects [3,4] revealed importance of REM sleep

Age Variation of the Tyrosine Hydroxylase Activities of the Terminal of the Caudate nucleus vs the Clinical Course of HPD
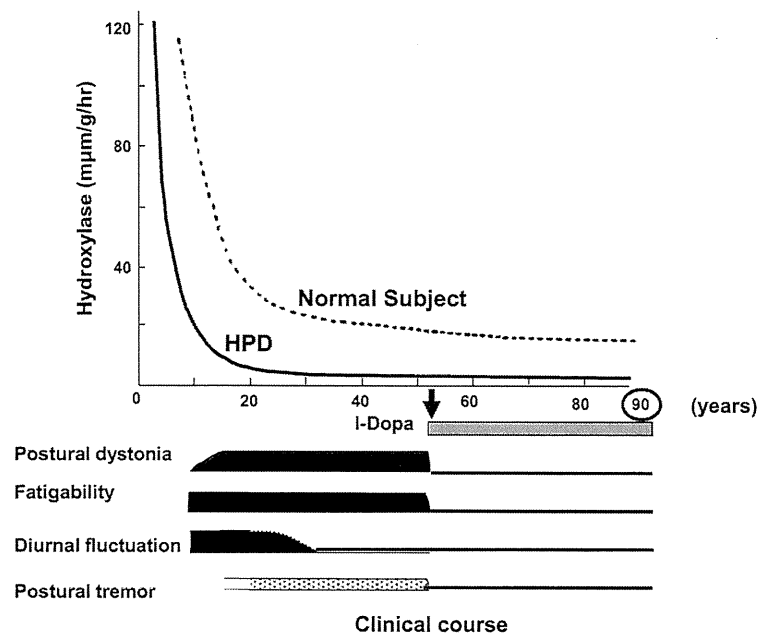

Fig. 1. Correlation of the 43 years clinical course of 51 years female postural type, with onset at 8 years and the age variation of the tyrosine hydroxylase activities of the terminals of the nigrostriatal dopamine neuron as the causative nucleus shown by McGeer and McGeer [9]. This case was completely recovered by L-dopa started at 51 years which continued without any side effects until 90 years.

(sREM) for the sleep effects by selective sleep stage deprivation studies [1]. Twitch movements (TMs) in sREM reflect the dopamine (DA) activities. In normal subjects TMs in sREM increase with sleep cycle and decrease with age. Degree of increment with sleep cycle reduces with age. The TMs of HPD patients followed these nocturnal and age variation with the lower levels of around 20% of normal values. In sREM of the 1st cycle it was markedly decreased less than 20% of the level in the last cycle of normal subjects, but in that of last cycle it exceeded more than 20%, which related morning recovery. Other parameters modulated by the brainstem aminergic neurons were preserved normally [3,4].

Fujita and Shintaku [10] revealed marked decrease less than 20% of the normal range of biopterin and neopterin in cerebrospinal fluid (CSF) of a case with HPD, by Furukawa et al. [11] confirmed the results and deficiency of GCH-1 was clarified as the cause of HPD [11]. In asymptomatic carriers these were 30–50% of normal levels. The activities of GCH-1 in the mononuclear blood cells decreased to less than 20% of normal levels in patients and 30–40% in asymptomatic carriers [2].

Ichinose found the gene of GCH-1 on 14q22.1 to q22.2 and examining seven HPD patients reveled this gene as the causative gene of HPD [2].

Neuroimaging, neurophysiological, neuropathological and neurohistological studies confirmed the pathophysiology speculated from clinical studies.

Magnetic resonance imaging (MRI) studies performed in various institutions revealed no abnormalities [3,4]. Brain positron emission tomography (PED) scans studies showed no definite abnormalities in [18F] dopa uptake, [11C] raclopride PET, [11C] N-spiperone PET [3] and normal development of the D_2 receptors in HPD [3,4]. In our experience of two 38 years, female patients of action type with 30 years' clinical courses without treatments after the onset at 8 years, and one 59 years male with onset at 58 years showed normal [18F] dopa uptake and [11C] N-spiperone PET. These confirmed decrease of TH as the cause of DA deficiency.

Evaluations of voluntary saccades revealed abnormalities in both visually guided (VGS) and memory guided saccades (MGS), and implicated involvement of both the direct and the indirect pathways of the basal ganglia [12]. In adult onset patients abnormalities were observed only in MGS.

Paired pulse transcranial magnetic stimulation was studied in two institutes [13,14]. One study showed residual abnormalities in motor inhibition in levodopa-treated HPD patients even though clinically asymptomatic [13]. However, the other study revealed that dysfunction of GABAa inhibitory interneurons of the primary motor cortex does not contribute to the generation of postural dystonia of HPD [14]. Sensory evoked potential revealed normal gating in patients with postural type, while it was abnormal in patients with action type.

These neurophysiological studies revealed involvement of the striatal direct pathway and the descending output of the basal ganglia for the postural type and the indirect pathway and the ascending pathway for tremor and symptoms of action type dystonia.

Neuropathological and neurohistochemical studies were performed on a case with action dystonia reported as juvenile parkinsonism [8] and a 19 years old DRD female, postural type died by traffic accident [15], both of which were later confirmed GCH-1 gene mutation.

Neuropathological examinations revealed decrease in melanin, particularly in the ventral tier of the pars compacta of the substantia nigra (SNc) [8,15], and one with morphological immaturity of the neurons [8]. Histochemically, DA content was subnormal [16] or normal [8] in the SNc, while it showed marked decrement in the striatum [8,16]. The reduction was greater in the putamen than in the caudate nucleus, and subregionally, the decrement was more great in the rostral caudate and the caudal putamen similar to PD. However, in contrast to PD this case showed a greater DA loss in the ventral subdivision of the rostral caudate, the area rich in striosome, than its dorsal counterpart, though in the putamen, the dorsoventral DA gradient was similar to PD [16]. The activity and protein content of TH was decreased in the striatum, but within normal range in the SNc [16].

Furukawa et al. [17] showed marked reduction of total biopterin (84%) and neopterin (62%) in the putamen, despite normal concentration of aromatic acid decarboxylase, DA transporter and vesicular monoamine transporter. These authors [18] also demonstrated modest reduction of TH protein (52%) and DA (44%), despite marked reduction of striatal biopterin (82%) in an asymptomatic carrier, and implicated the levels of TH protein as a key for development of symptoms.

Up to now more than one hundred independent mutations have been identified in the coding region of GCH-1 which is identical in one family, but differs among families [2–4]. However, we found two occasions showing identical mutation in unrelated families.

It was shown molecular analysis remains unable to determine mutations in the coding region of the gene in approximately 40% of subjects with GCH-1 deficiency. In these cases, abnormalities in intron genomic deletion, a large gene deletion, an intragenic duplication or inversion of GCH-1 or mutation in as yet undefined regulatory gene modifying enzyme function may be present [3,4].

4. Pathophysiological consideration

As for the pathogenetic mechanisms for dominant inheritance with heterozygous mutation, classic dominant negative effects have been considered [3,4]. The rates of mutant GCH-1 messenger ribonucleic acid (mRNA) production against normal mRNA were 28% in a patient but 8.3% in an asymptomatic carrier [3,4]. However, the ratio varies depending on the locus of the mutation. Furthermore, the ratio differed among affected individuals in some families. These may cause inter- and intra-familial variation of the phenotype as well as the rate of penetrance. Furthermore, the loci of the mutation may also be involved in phenotype.

It is also necessary why a certain mutation relate particular clinical symptoms shown above.

As the enzyme for the synthesis of BH$_4$, GCH-1 deficiency may affect tryptophan hydroxylase (TPH) as well as TH. There is the difference of K_m value for TH and TPH. With heterozygous mutant gene, the BH$_4$ decreases partially in HPD. Thus TH with higher affinity to BH$_4$ is affected rather selectively [3,4]. However, in molecular conditions with marked decrease of BH$_4$, TPH is affected as well as TH and may produce symptoms induced by deficiencies of the 5HT neurons.

In basal ganglia disorders, contralateral or ipsilateral of the side of predominantly involved of the sternocleidomastoideus (SCM) and the extremities reflects the region of the causative lesion.

In postural type of AD GCH-1 deficiency, predominant side of rigid hypertonus is contralateral between the SCM and the extremities. This suggests the lesion in the afferent structure to the striatum with side predominance ipsilateral to the predominantly affected side of the SCM, that is, involvement of the NS DA neuron with predominance to the side predominantly affected SCM.

Postural tremor, torticollis and generalized rigid hypertonus develop later independently from postural dystonia. The side predominance of these symptoms is ipsilateral both in the extremities and in the SCM. This implicates a causative lesion located in the downstream of the striatum. As these symptoms are DA responsive, it is suggested that hypofunction of the DA neuron projecting to the D$_1$ receptor on the subthalamic nucleus (STN) is postulated to be involved [3,4].

Furthermore, results of the stereotactic surgeries and the paired pulse transcranial magnetic stimulation show involvement of the ascending output of the basal ganglia in tremor, focal and segmental dystonia and rigidity in adult onset cases. These processes are also involved in focal dystonia.

Whereas, dopa-responsive growth arrest seen in children with HPD postulates the involvement of D$_4$ receptor of the tuberoinfundibular tract. The D$_4$ receptor belongs to the D$_2$ receptor family, which matures early among D$_2$ families [3,4]. This implicates that the terminals of the NS-DA neuron in HPD connect to the receptors which develop early.

Pteridine metabolism develops in late fetal period with critical period in early infancy which extends to

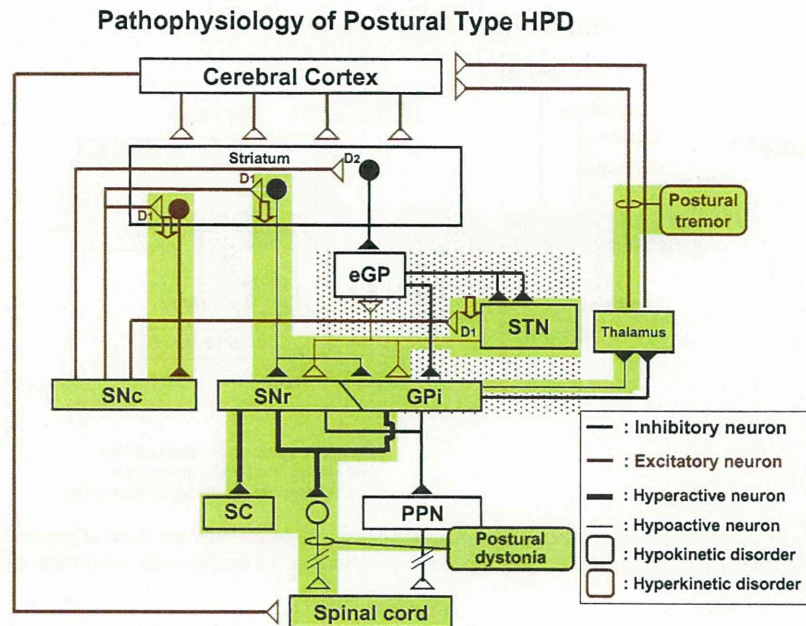**Pathophysiology of Postural Type HPD**

Fig. 2. Pathophysiologies of HPD; GPe: globus pallidus external segment; GPI: globus pallidus internal segment; STN: subthalamic nucleus; SNc: substantia nigra pars compacta; SN: substantia nigra pars reticula; SC: superior colliculus; PPN: pedunculopontine nucleus.
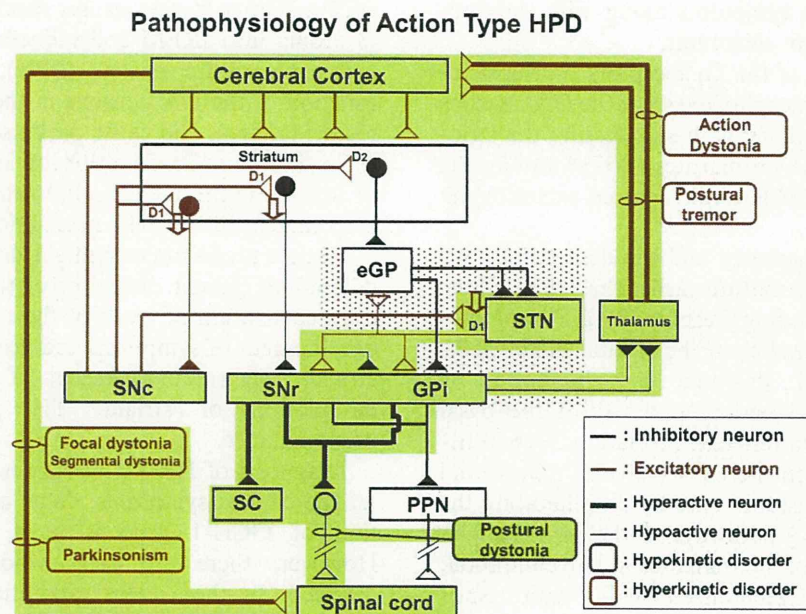
Pathophysiology of Action Type HPD

Fig. 3. Pathophysiologies of HPD; GPe: globus pallidus external segment; GPi: globus pallidus internal segment; STN: subthalamic nucleus; SNc: substantia nigra pars compacta; SN: substantia nigra pars reticula; SC: superior colliculus; PPN: pedunculopontine nucleus.

early childhood [19]. Study in stimulated mononuclear blood cells [20] also showed age-dependent decrement of the activities of GCH-1 in the first three decades of life. Thus pteridine metabolism may involve in the age related decrement of TH activity [10] particularly in its early phase.

Thus, the pathophysiologies of postural and action type dystonia of HPD are shown in **Figs. 2 and 3**.

GCH-1 deficiency caused by abnormalities of pteridine metabolism leads to the decrease of the TH protein or DA in the ventral area of the striatum or the striosome in early developmental course.

M. Segawa / Brain & Development 33 (2011) 195–201
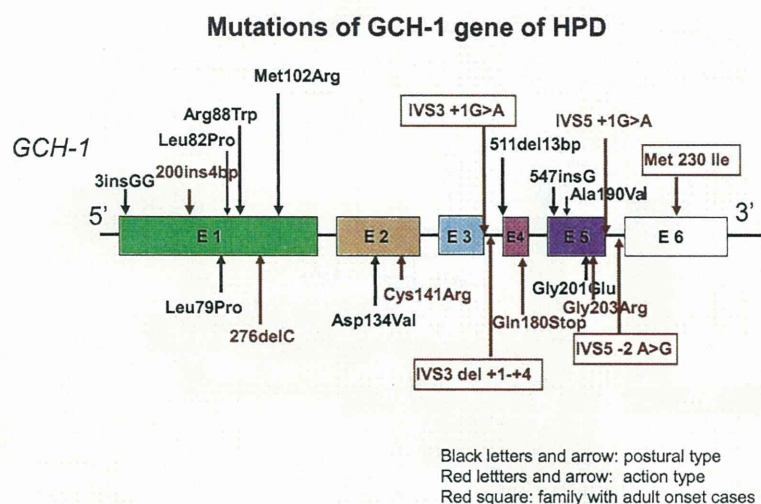
Mutations of GCH-1 gene of HPD

Fig. 4. Locus of the mutation of the GCH-1 gene in HPD. The mutations shown with black letter are those of postural type, these shown with red letters are mutations of action type. Those surrounded by red square are mutations of the families with adult onset cases.

The D_1 DA receptors develop early among DA receptors. Thus, in HPD deficiency of TH or DA at the terminal of the NS DA neuron projecting to the D_1 receptors provides characteristic symptoms along with development of the downstream structures.

Thus disfacilitation of the D_1 receptors on the striosome causes failure in morphogenesis of the DA neurons in the SNc by early infancy with suppressing the striosome–SNc pathway, which matures earliest among the striatal outputs, with GABAergic neuron, excitatory at the age.

The striatal direct pathway and the descending output of the basal ganglia mature earlier than the indirect pathway and the ascending outputs [3,4]. Thus hypofunction of the D_1 receptor on the striatal direct pathway causes postural dystonia in childhood by disinhibition of the descending pathway of the basal ganglia to the brainstem reticular formation. Hypofunction of DA terminals on the STN provides tremor and symptoms of action dystonia type by disfacilitating the late maturing ascending pathways of the basal ganglia to the specific nucleus of the thalamus in late childhood, and focal dystonia and generalized rigidity with tremor in adulthood [4].

Postural dystonia is a hypokinetic disorder, while the action dystonia and other symptoms related to the STN are hyperkinetic disorders.

However, it is not clarified why these pathophysiologies develop under normal DA activities in the SNc.

Postural type and action type are differed by the mutation (**Fig. 4**). But there observed no particular coding region for these types.

Failure in development and modulation of postural tone and locomotion and psychobehavioral function from early infancy observed in compound heterozygotes and early onset phenotypes are considered to be caused by deficiency of 5HT activities. The deficiency of the 5HT activities further causes insufficiency in restriction of atonia into sREM and induces hypofunction of the pedunculopontine nucleus (PPN), which induce hypofunction of the DA neurons in the SNc and the ventro tegmental area, and cause parkinsonian and psychological symptoms. Preservation of interlimb coordination or locomotion in classic HPD suggests minimum or no involvement of the 5HT neuron [4].

Female predominance might depend on a genetically determined gender difference of the DA neuron. However, correlation of levels of the striatal TH protein for development of symptoms and gender difference in penetrance, suggest involvement of gender difference in modulation of striatal TH protein for female predominance.

Diagnosis of HPD is usually not difficult by characteristic clinical symptoms. Gene analysis for the mutation of GCH-1 gene is most definitive diagnosis. However, there are cases whose mutation is not detected. In these cases estimation of neopterin and biopterin in CSF, and GCH-1 activity in peripheral mononuclear cells are reliable.

A part of this study was presented at the 10th Asian and Oceanian Congress of Child Neurology which was held in Daegu, Korea, June 10–13, 2009.

References

[1] Segawa M, Hosaka A, Miyagawa F, Nomura Y, Imai H. Hereditary progressive dystonia with marked diurnal fluctuation. Adv Neurol 1976;14:215–33.

[2] Ichinose H, Ohye T, Takahashi E, Seki N, Hori T, Segawa M, et al. Hereditary progressive dystonia with marked diurnal fluctuation caused by mutations in the GTP cyclohydrolase I gene. Nat Genet 1994;8:236–42.

[3] Segawa M. Hereditary progressive dystonia with marked diurnal fluctuation. Brain Dev 2000;22:S65–80.

[4] Segawa M, Nomura Y, Nishiyama N. Autosomal dominant guanosine triphosphate cyclohydrolase I deficiency (Segawa disease). Ann Neurol 2003;54:S32–45.

[5] Furukawa Y, Lang AE, Trugman JM, Bird TD, Hunter A, Sadeh M, et al. Gender-related penetrance and de novo GTP-cyclohydrolase I gene mutations in dopa-responsive dystonia. Neurology 1998;50:1015–20.

[6] Segawa M, Nomura Y, Yamashita S, Kase M, Nishiyama N, Yukishita S, et al. Long-term effects of L-dopa on hereditary progressive dystonia with marked diurnal fluctuation. In: Berardelli A et al., editors. Motor disturbances II. London: Academic Press; 1990. p. 305–18.

[7] Segawa M, Nomura Y, Takita K, Narabayashi H. Pallidotomy and thalamotomy on a case with hereditary progressive dystonia with marked diurnal fluctuation. Mov Disord 1998;13:S165.

[8] Narabayashi H, Yokochi M, Iizuka R, Nagatsu T. Juvenile Parkinsonism. In: Vinken PJ, Bruyn GW, Klawans HL, editors. Handbook of clinical neurology, vol. 5(49), extrapyramidal disorders. Amsterdam: Elsevier Science Publishers B.V; 1986. p. 153–65.

[9] McGeer EG, McGeer PL. Some characteristics of brain tyrosine hydroxylase. In: Mandel J, editor. New concepts in neurotransmitter regulation. New York, London: Plenum; 1973. p. 53–68.

[10] Fujita S, Shintaku H. Etiology and pteridine metabolism abnormality of hereditary progressive dystonia with marked diurnal fluctuation (HPD: Segawa disease). Med J Kushiro City Hosp 1990;2:64–7.

[11] Furukawa Y, Nishi K, Kondo T, Mizuno Y, Narabayashi H. CSF biopterin levels and clinical features of patients with juvenile Parkinsonism. Adv Neurol 1993;60:562–7.

[12] Hikosaka O, Fukuda H, Kato M, Uetake K, Nomura Y, Segawa M. Deficits in saccadic eye movements in hereditary progressive dystonia with marked diurnal fluctuation. In: Segawa M, editor. Hereditary progressive dystonia with marked diurnal fluctuation. UK: The Parthenon Publishing Group; 1993. p. 159–77.

[13] Huang YZ, Trender-Gerhard I, Edwards MJ, Mir P, Rothwell JC, Bhatia KP, et al. Motor system inhibition in dopa-responsive dystonia and its modulation by treatment. Neurology 2006;66:1088–90.

[14] Hanajima R, Nomura Y, Segawa M, Ugawa Y. Intracortical inhibition of the motor cortex in Segawa disease (DYT5). Neurology 2007;68:1039–44.

[15] Rajput AH, Gibb WR, Zhong XH, Shannak KS, Kish S, Chang LG, et al. Dopa-responsive dystonia: pathological and biochemical observations in a case. Ann Neurol 1994;35:396–402.

[16] Hornykiewicz O. Striatal dopamine in dopa-responsive dystonia comparison with idiopathic Parkinson's disease and other dopamine-dependent disorders. In: Segawa M, Nomura Y, editors. Age-related dopamine-dependent disorders. Monogr Neural Sci, vol. 14. Basel: Karger; 1995. p. 101–8.

[17] Furukawa Y, Nygaard TG, Gütlich M, Rajput AH, Pifl C, DiStefano L, et al. Striatal biopterin and tyrosine hydroxylase protein reduction in dopa-responsive dystonia. Neurology 1999;53:1032–41.

[18] Furukawa Y, Kapatos G, Haycock JW, Worsley J, Wong H, Kish SJ, et al. Brain biopterin and tyrosine hydroxylase in asymptomatic dopa-responsive dystonia. Ann Neurol 2002;51:637–41.

[19] Shintaku H. Early diagnosis of 6-pyruvoyl-tetrahydropterin synthase deficiency. Pteridines 1994;5:18–27.

[20] Hibiya M, Ichinose H, Ozaki N, Fujita K, Nishimoto T, Yoshikawa T, et al. Normal values and age-dependent changes in GTP cyclohydrolase I activity in stimulated mononuclear blood cells measured by high-performance liquid chromatography. J Chromatogr B Biomed Sci Appl 2000;740:35–42.

Congenital Dysplastic Microcephaly and Hypoplasia of the Brainstem and Cerebellum With Diffuse Intracranial Calcification

Kazuyuki Nakamura, MD, Mitsuhiro Kato, MD, PhD,
Ayako Sasaki, MD, PhD, Masayo Kanai, MD, PhD, and
Kiyoshi Hayasaka, MD, PhD

Abstract

Congenital microcephaly with intracranial calcification is a rare condition presented in heterogeneous diseases. Here, we report the case of a 1-year-old boy with severe congenital microcephaly and diffuse calcification. Neuroimaging studies showed a diffuse simplified gyral pattern; a very thin cortex; ventricular dilatation; very small basal ganglia, thalamus, and brainstem; and cerebellar hypoplasia with diffuse calcification. Clinical features of intrauterine infections, such as neonatal jaundice, hepatomegaly, and thrombocytopenia, were not found. Serological tests, cultures, and polymerase chain reaction analysis were negative for viral infections. The etiology of pseudo–toxoplasmosis, rubella, cytomegalovirus, and herpes simplex syndrome is still unknown. This study describes the most severe form of pseudo–toxoplasmosis, rubella, cytomegalovirus, and herpes simplex syndrome reported to date, with the patient showing microcephaly and calcification or band-like intracranial calcification with simplified gyration and polymirogyria.

Keywords

microcephaly, intracranial calcification, pontocerebellar hypoplasia, toxoplasmosis, rubella, cytomegalovirus, herpes simplex

Congenital microcephaly with brain dysgenesis and intracranial calcification is a characteristic feature of intrauterine infections of toxoplasma, rubella, cytomegalovirus, herpes virus, and other infectious agents, including human immunodeficiency virus and the bacteria that cause syphilis. This form of congenital microcephaly has been termed the toxoplasmosis, rubella, cytomegalovirus, and herpes simplex syndrome.[1] In addition to congenital microcephaly and intracranial calcification, toxoplasmosis, rubella, cytomegalovirus, and herpes simplex syndrome shows systemic abnormalities, such as thrombocytopenia, anemia, hepatosplenomegaly, liver dysfunction, jaundice, and chorioretinitis, with elevated serum immunoglobulin M (IgM) levels at birth. Similar clinical conditions have been reported in several patients with familial occurrence but with no evidence of infection. These clinical conditions have been designated as "pseudo–toxoplasmosis, rubella, cytomegalovirus, and herpes simplex" syndrome.[2] In addition, "band-like intracranial calcification with simplified gyration and polymicrogyria" has also been reported. However, this syndrome shows no evidence of infection, abnormalities in liver function, or thrombocytopenia.[3,4]

It is important to discriminate these syndromes for genetic counseling. This report describes a patient with congenital microcephaly and whole brain dysgenesis and extensive calcification, suggesting a severe form of pseudo–toxoplasmosis, rubella, cytomegalovirus, and herpes simplex syndrome, or band-like intracranial calcification with simplified gyration and polymicrogyria.

Case Report

The boy was born to healthy, unrelated, 29-year-old Japanese parents. This was the mother's first pregnancy, and the boy had no siblings. There were no household pets including cats. During the 5- to 6-week period of gestation, his mother had fever for 1 day but showed no other symptoms. Microcephaly was first observed on ultrasound examination conducted at 28 weeks of gestation. At 34 weeks of gestation, specific IgMs

Department of Pediatrics, Yamagata University Faculty of Medicine, Yamagata, Japan

Corresponding Author:
Kazuyuki Nakamura, MD, Department of Pediatrics, Yamagata University Faculty of Medicine, 2-2-2, Iida-Nishi, Yamagata 990-9585, Japan
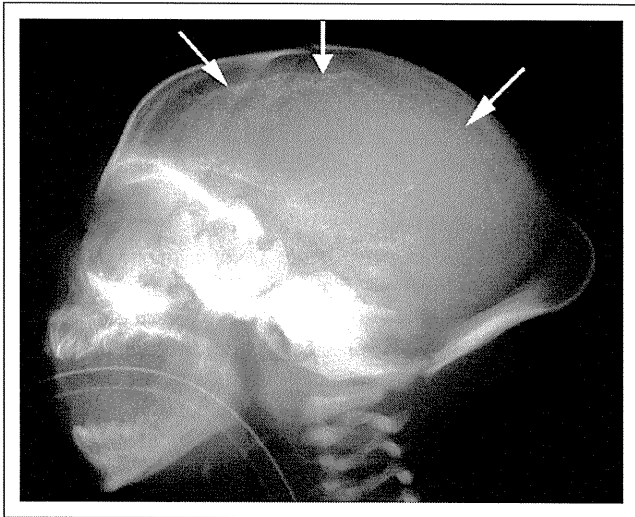Email: kazun-yamagata@umin.ac.jp

Figure 1. A plain radiograph of the head shows the cranial vault with a frontal sloping and a marked external occipital protuberance. Intracranial high-density spots are visible along the cerebral wall (arrows).

against rubella, cytomegalovirus, and toxoplasma were negative in the mother. He was delivered by caesarean section because of hypotonic uterine dysfunction at 42 weeks of gestation. His Apgar score was 1 at 1 min. He required intratracheal intubation for severe dyspnea. His weight at birth was 3140 g; length, 46 cm (−2.0 SD); and head circumference, 29 cm (−3.2 SD). He had bilateral undescended testis without hepatosplenomegaly or a petechial rash. Ophthalmologic examination showed no corneal clouding or chorioretinitis. Neurological examination showed the presence of hypotonic muscles and absence of a Moro reflex. Skull radiography showed a sloping forehead and several intracranial calcific densities (Fig. 1). A computed tomographic (CT) scan of the head showed prominent calcification mainly along the ventricular wall from the cerebrum to the brain stem (Fig. 2). Magnetic resonance imaging (MRI) of the brain showed severe diffuse simplified gyri combined with a thinning of the cortex and the white matter; marked dilated ventricles; and severe hypoplasia of the basal ganglia, thalamus, cerebellum, and brainstem (Fig. 3). At the age of 4 days, a hematological examination (hemoglobin, 18.3 g/dL; white blood cells, 10 010/μL; neutrophils, 69%; platelets, 32.8 × 10^4/μL^3) and blood chemistry tests, including those for calcium, phosphate, aspartate aminotransferase, alanine aminotransferase, lactate, and amino acids were normal. The total serum IgM was 8 mg/dL; the specific IgMs against toxoplasma, rubella, cytomegalovirus, herpes simplex, and varicella-zoster virus were negative. Viral cultures of a pharyngeal swab and urine were negative. Subsequent polymerase chain reaction (PCR) amplification of cytomegalovirus DNA in urine and the umbilical cord was also negative. An antibody titer for lymphocytic choriomeningitis virus was negative. G-banding chromosomal analysis showed a karyotype of 46, XY. At the age of 10 months, a cerebrospinal fluid examination did not show increased number of lymphocytes or interferon-alpha.

Figure 2. Computed tomographic scan of the head shows linear or patchy high signals consisting of calcifications within or immediately beneath the cortex and the enlargement of the lateral ventricles.

Electroencephalography showed multifocal sharp waves with low-voltage background activity. At 12 months of age, he showed hypothermia (<36°C); recurrent urinary tract infections caused by vesicoureteral reflux; and a profound developmental delay with limb contractures, no eye contact, and no head control. He received tube feeding because of bulbar palsy.

Discussion

Congenital microcephaly results from various clinical conditions such as infections, radiation, exogenous toxic agents, anoxic or metabolic insults, and genetic bases.[1] Although these conditions can also cause cerebral calcification, the association of congenital microcephaly and calcification are rare. Our patient experienced a febrile episode, suggesting an infection at 5 to 6 weeks of gestation, but there was no history of any other insult. Since intrauterine infections or toxoplasmosis, rubella, cytomegalovirus, and herpes simplex syndrome, especially cytomegalovirus infection, is the most frequent cause of congenital microcephaly and since calcification and earlier infection induce severer brain anomalies,[1] we tried to obtain evidence of a prenatal infection of cytomegalovirus using serological tests, cultures, and PCR amplification. However, none of these tests yielded a positive result, which could be a result of early infection during fetal development. The fetus showed no immunological response, and the virus could not be cultured. Moreover, the PCR sensitivity was sufficiently high enough to detect viral DNA.[5] On
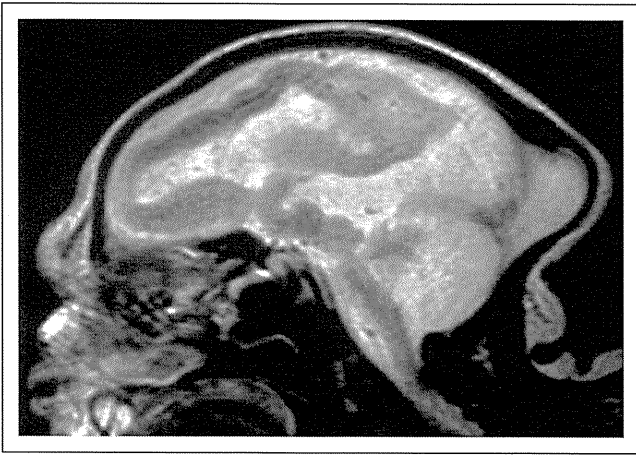
Figure 3. Sagittal T2-weighted magnetic resonance imaging (MRI) shows a thin cortex and white matter with an undetectable border. Prominent hypoplasia of the cerebellum and brainstem is visible.

the basis of these results, we conclude that cytomegalovirus is unlikely to be the cause of our patient's condition.

During the middle embryonic period (5–6 weeks of gestation in humans), secondary brain vesicles (telencephalon, diencephalon, mesencephalon, metencephalon, and myelencephalon) are formed; the primitive cerebral hemispheres develop during neuronogenesis in the ventricular zone. Insult at this stage can engender extremely severe brain malformation (eg, decreased brain size) because of the inhibition of cell proliferation and the dysplastic configuration of the brain that results from impaired cell migration. The hypoplastic brainstem and cerebellum as well as microcephaly with the thin cortex and irregular convolution seen in our patient suggest an event during early embryogenesis, although the etiology is unknown.

Although our patient showed an irregular convolution that suggested possible cortical dysplasia, the very thin cortex suggested microcephaly with normal to thin cortex or microcephaly with a simplified gyral pattern.[6] To date, 5 genes (*MCPH1, ASPM, CDK5RAP2, CENPJ,* and *SLC25A19*) have been found to be responsible for the autosomal recessive inheritance of microcephaly with a simplified gyral pattern.[7,8] Mutations in these genes result in congenital microcephaly but not in a calcification resembling the one in our patient. Microcephaly with polymicrogyria or other cortical dysplasias or microcephaly with pontocerebellar hypoplasia are other candidate conditions for our patient, but neither one shows calcification.[9] At this point, it is difficult to categorize the neuroimaging features of our patient into the classification scheme for malformations of cortical development.[6]

Aicardi–Goutières syndrome is an autosomal recessive form of progressive encephalopathy characterized by acquired microcephaly, leukodystrophy, and calcifications of the basal ganglia, which is similar to toxoplasmosis, rubella, cytomegalovirus, and herpes simplex syndrome.[10] Recently, 5 genes (*TREX1, RNASEH2B, RNASEH2C, RNASEH2A,* and *SAMHD1*) have been identified as the responsible genes for this syndrome.[11-13] Elevated interferon-alpha levels and chronic

lymphocytosis in the cerebrospinal fluid are specific features of Aicardi–Goutières syndrome. However, our patient had neither of these features. Although cerebrospinal fluid lymphocytosis is not necessary for an Aicardi–Goutières syndrome diagnosis[14] and although a small number of patients show microcephaly at birth, the cerebral dysplasia observed in our patient has never been reported as a manifestation of Aicardi–Goutières syndrome.

It has been suggested that pseudo–toxoplasmosis, rubella, cytomegalovirus, and herpes simplex syndrome is the same disorder as Aicardi–Goutières syndrome.[15] Periventricular areas are commonly calcified in pseudo–toxoplasmosis, rubella, cytomegalovirus, and herpes simplex syndrome, but the basal ganglia, cerebellum, and brainstem can also be affected. Brain MRIs often show cerebral atrophy, enlarged lateral ventricles, and severe hypoplasia of the corpus callosum, cerebellum, and brainstem. Some patients also show associated cortical dysplasia.[2,16] One report described a patient as having microcephaly with plate-like cortical calcification and with an extremely decreased convolution of the cerebral cortex, which is similar to our patient's condition.[17] However, the brainstem and cerebellum were spared in that patient.

Band-like intracranial calcification with simplified gyration and polymicrogyria is inherited as an autosomal recessive trait, and mutations of the *OCLN* gene have been identified as resulting in this condition.[18] Band-like intracranial calcification with simplified gyration and polymicrogyria is similar to pseudo–toxoplasmosis, rubella, cytomegalovirus, and herpes simplex syndrome in that both show widespread intracranial calcification and polymicrogyria and that some patients show hypoplasia of the cerebellum and brainstem. There are differences between these 2 conditions in terms of the postnatal microcephaly, the characteristic band-like calcification, and the lack of evidence for neonatal disturbance of liver function with thrombocytopenia; nonetheless, they can have similar etiologies.[3,4]

The extensive lesions of the brain are reminiscent of multicystic encephalomalacia, which are often accompanied by extensive dystrophic calcifications in zones of infarction. Multicystic encephalomalacia is also caused by fetal viral infection as well as hypoxia or circulatory insults; however, the lesions in the patient appeared to be too broad for secondary injury and had no visible cysts, as observed by MRI. The size and number of cysts depends on the stage of infarction, which can be both of major cerebral vessels and of the microcirculation at capillary levels.[19] Neuropathological confirmation is essential to reveal the pathogenesis.

It is noteworthy that this is the most severe case of a patient with congenital dysplastic microcephaly and brainstem and cerebellar hypoplasia with extensive intracranial calcification. The pathogenesis, particularly regarding its inheritance, remains to be clarified.

Acknowledgments

References

1. Volpe JJ. In: *Neurology of the Newborn*. 5th ed. Philadelphia, PA: WB Saunders;; 2008.

2. Vivarelli R, Grosso S, Cioni M, et al. Pseudo-TORCH syndrome or Baraitser-Reardon syndrome: diagnostic criteria. *Brain Dev.* 2001;23:18-23.

3. Briggs TA, Wolf NI, D'Arrigo S, et al. Band-like intracranial calcification with simplified gyration and polymicrogyria: a distinct "pseudo-TORCH" phenotype. *Am J Med Genet A*. 2008;146: 3173-3180.

4. Abdel-Salam GM, Zaki MS, Saleem SN, Gaber KR. Microcephaly, malformation of brain development and intracranial calcification in sibs: pseudo-TORCH or a new syndrome. *Am J Med Genet A*. 2008;146:2929-2936.

5. Revello MG, Zavattoni M, Furione M, et al. Diagnosis and outcome of preconceptional and periconceptional primary human cytomegalovirus infections. *J Infect Dis*. 2002;186:553-557.

6. Barkovich AJ, Kuzniecky RI, Jackson GD, et al. A development and genetic classification for malformations of cortical development. *Neurology*. 2005;65:1873-1887.

7. Rosenberg MJ, Agarwala R, Bouffard G, et al. Mutant deoxynucleotide carrier is associated with congenital microcephaly. *Nat Genet*. 2002;32:175-179.

8. Woods CG, Bond J, Enard W. Autosomal recessive primary microcephaly (MCPH): a review of clinical, molecular, evolutionary findings. *Am J Hum Genet*. 2005;76:717-728.

9. Hashimoto K, Takeuchi Y, Kida Y, et al. Three siblings of fatal infantile encephalopathy with olivopontocerebellar hypoplasia and microcephaly. *Brain Dev*. 1998;20:169-174.

10. Goutières F. Aicardi-Goutières syndrome. *Brain Dev*. 2005;27: 201-206.

11. Crow YJ, Leitch A, Hayward BE, et al. Mutations in genes encoding ribonuclease H2 subunits cause Aicardi-Goutières syndrome and mimic congenital viral brain infection. *Nat Genet*. 2006;38: 910-916.

12. Crow YJ, Hayward BE, Parmar R, et al. Mutations in the gene encoding the 3'-5' DNA exonuclease TREX1 cause Aicardi–Goutières syndrome at the AGS1 locus. *Nat Genet*. 2006;38: 917-920.

13. Rice GL, Bond J, Asipu A, et al. Mutations involved in Aicardi–Goutières syndrome implicate SAMHD1 as regulator of the innate immune response. *Nat Genet*. 2009;41:829-832.

14. Crow YJ, Black DN, Ali M, et al. Cree encephalitis is allelic with Aicardi-Goutières syndrome: implications for the pathogenesis of disorders of interferon alpha metabolism. *J Med Genet*. 2003;40: 183-187.

15. Sanchis A, Cerveró L, Bataller A, et al. Genetic syndromes mimic congenital infections. *J Pediatr*. 2005;146:701-705.

16. Burn J, Wickramasinghe HT, Harding B, Baraitser M. A syndrome with intracranial calcification and microcephaly in two sibs, resembling intrauterine infection. *Clin Genet*. 1986; 30:112-116.

17. Kalyanasundaram S, Dutta S, Narang A, Katariya S. Microcephaly with plate-like cortical calcification. *Brain Dev*. 2003;25: 130-132.

18. O'Driscoll MC, Daly SB, Urquhart JE, et al. Recessive mutations in the gene encoding the tight junction protein occludin cause band-like calcification with simplified gyration and polymicrogyria. *Am J Hum Genet*. 2010;87:354-364.

19. Weiss JL, Cleary-Goldman J, Tanji K, et al. Multicystic encephalomalacia after first-trimester intrauterine fetal death in monochorionic twins. *Am J Obstet Gynecl*. 2004;190: 563-565.

Dandy–Walker Malformation Associated With Heterozygous *ZIC1* and *ZIC4* Deletion: Report of a New Patient

Jun Tohyama,[1,2]* Mitsuhiro Kato,[3] Sari Kawasaki,[4] Naoki Harada,[5] Hiroki Kawara,[5] Takeshi Matsui,[5] Noriyuki Akasaka,[1] Tsukasa Ohashi,[1] Yu Kobayashi,[1] and Naomichi Matsumoto[6]

[1]Department of Pediatrics, Nishi-Niigata Chuo National Hospital, Niigata, Japan

[2]Department of Pediatrics, Niigata University Medical and Dental Hospital, Niigata, Japan

[3]Department of Pediatrics, Yamagata University School of Medicine, Yamagata, Japan

[4]Department of Neurology, Saigata National Hospital, Jouetsu, Japan

[5]Department of Molecular Genetic Testing, Clinical Laboratory Center, Mitsubishi Chemical Medience Corporation, Nagasaki, Japan

[6]Department of Human Genetics, Yokohama City University Graduate School of Medicine, Yokohama, Japan

We report on a female patient with Dandy–Walker malformation possibly caused by heterozygous loss of *ZIC1* and *ZIC4*. The patient presented with mental retardation, epilepsy, and multiple congenital malformations including spina bifida, mild dysmorphic facial features including, thick eyebrows, broad nose, full lips, macroglossia, and hypoplasia of the cerebellar vermis with enlargement of the fourth ventricle on brain magnetic resonance imaging, which is consistent with Dandy–Walker malformation. A chromosome analysis showed interstitial deletion of chromosome 3q23-q25.1. Fluorescence in situ hybridization (FISH) and microarray-based genomic analysis revealed the heterozygous deletion of *ZIC1* and *ZIC4* loci on 3q24. Her facial features were not consistent with those observed in blepharophimosis–ptosis–epicanthus inversus syndrome (BPES) involving *FOXL2* abnormality. Other deleted genes at 3q23-25.1 might contribute to the dysmorphic facial appearance. A milder phenotype as the Dandy–Walker malformation in our patient supports the idea that modifying loci/genes can influence the development of cerebellar malformation. © 2010 Wiley-Liss, Inc.

Key words: Dandy–Walker malformation; interstitial deletion 3q; *ZIC1*; *ZIC4*

How to Cite this Article:

Tohyama J, Kato M, Kawasaki S, Harada N, Kawara H, Matsui T, Akasaka N, Ohashi T, Kobayashi Y, Matsumoto N. 2011. Dandy–Walker malformation associated with heterozygous *ZIC1* and *ZIC4* deletion: Report of a new patient.

Am J Med Genet Part A 155:130–133.

INTRODUCTION

Dandy–Walker malformation (DWM) is an abnormality in the development of the central nervous system that is defined by hypoplasia and upward rotation of the cerebellar vermis and cystic dilatation of the fourth ventricle [Hart et al., 1972; Parisi and Dobyns, 2003]. DWM is etiologically heterogeneous in association with a wide variety of chromosomal anomalies, various Mendelian disorders, multifactorial disorders, and environmental factors [Murray et al., 1985; Chitayat et al., 1994].

Grinberg et al. [2004] described seven nonrelated patients of DWM with de novo interstitial deletions of chromosome 3q. Cytogenetic investigation of these patients showed the first critical region involved in DWM, which encompasses genes *ZIC1* and *ZIC4*. There are five *Zic* genes encoding zinc finger proteins in humans and mice [Grinberg and Millen, 2005]. *ZIC1* and *ZIC4* are tightly linked on human chromosome 3 and mouse chromosome 9 [Grinberg et al., 2004; Grinberg and Millen, 2005]. A heterozygous deletion of these two linked genes in mice resulted in a phenotype that closely resembles DWM [Grinberg et al., 2004], strongly suggesting that heterozygous deletion of both *ZIC1* and *ZIC4* is the cause of DWM in humans. This is the second report on a new patient of DWM with heterozygous *ZIC1* and *ZIC4* deletion.

130